

LRP 690/01

February 2001

**Plasma Jet Properties in a New  
Spraying Process at Low Pressure for  
Large Area Thin Film Deposition**

J.-L. Drier, M. Gindrat, Ch. Hollenstein,  
M. Loch, A. Refke, A. Salito, G. Barbezat

## Plasma Jet Properties in a New Spraying Process at Low Pressure for Large Area Thin Film Deposition

*J. -L. Dorier, M. Gindrat, Ch. Hollenstein  
EPFL-CRPP, Lausanne, Switzerland*

*M. Loch, A. Refke, A. Salito, G. Barbezat  
Sulzer Metco (Switzerland) AG, Wohlen, Switzerland*

**Key words:** Optical spectroscopy, Enthalpy probe, LPPS-Thin Film, Supersonic plasma jet, Temperature and velocity, Plasma diagnostics

### Abstract

This paper describes an experimental investigation of plasma jet properties of a DC torch operated at low pressure (below 10 mbar). A modified enthalpy probe system is described, which allows gas sampling from the plasma jet at pressures down to the mbar range. Measurements of the specific enthalpy, temperature and velocity throughout the jet for different pressures are presented and discussed. In the pressure range investigated, the jet flow is supersonic and compressible theory is used to infer the velocity from the dynamic pressure measured at the probe tip. In addition, optical emission spectroscopy of the plasma jet is used to evidence the differences of these low-pressure plasmas with respect to common, atmospheric pressure thermal jets. These preliminary measurements are the starting points towards a better understanding of plasma jets at low operating pressures in view of new process development and optimisation.

### Introduction

Thermal spray coating using plasma torches either in ambient or controlled atmosphere is a well-established technology that is successfully applied in particular in the aeronautics, gas turbine and automotive industries [1]. In these processes, the plasma jet is intrinsically limited in size, which disqualifies them for coating large substrates uniformly in a reasonable time. Recently, a new process (Low Pressure Plasma Spraying-Thin Film [2]) which uses a plasma torch operating at low pressure has been developed with the aim of depositing uniform thin layers on large surfaces. Applications cover deposition of thin layers of metal oxide or other materials on large sheets in a single shot [3]. This new process is able to bridge the gap between conventional CVD/PVD thin film deposition and thick, thermally sprayed deposits. Because of the large pressure difference between the inside and the outside of the plasma gun, the exiting plasma jet experiences unconventional behaviour related to supersonic expansion at reduced pressure.

Moreover at low pressures, the collision rate is strongly decreased and the plasma jet may no longer be in local thermodynamic equilibrium [4]. Therefore its properties, in particular the temperature of the electrons and of the heavy species, the specific enthalpy, the velocity and turbulence remain to be determined.

Previous experimental investigations of the plasma jet from torches used for plasma spraying at reduced pressures were limited down to the 100 mbar pressure range [5]. Another kind of expanding plasma jet at low pressure, generated by a cascaded-arc torch [6] has been extensively investigated experimentally and modeled. But this covers the pressure range below 1 mbar and it is used for thin film deposition from gas and not for spraying because of the lack of local heat flux to melt solid particles.

The enthalpy probe technique, originally developed in the 1960's, is currently extensively used for the diagnostics of thermal plasma jets in spraying processes at atmospheric pressure [7, 8]. Its main advantages are the simplicity of the technique and the possibility to obtain simultaneous measurement of multiple plasma parameters such as enthalpy, temperature, velocity, density and composition, with a reasonable spatial resolution. The main disadvantages are the lack of time resolution and the fact that it is an intrusive diagnostic. A common enthalpy probe system has been used to investigate an induction plasma torch equipped with supersonic nozzles by Hollenstein et al. [9] down to about 170 mbar. The enthalpy probe performance in compressible plasma jets has been investigated by Fincke and co-workers [10], by comparison with light scattering measurements for sub- and supersonic flows.

In this paper a modified enthalpy probe system, which allows measurements down to a chamber pressure of 2 mbar, is described and preliminary results are presented.

**Experimental arrangement**

The plasma gun (Fig. 1) investigated here is a Sulzer Metco O3CP which is operated inside a vacuum vessel for "Low Pressure Plasma Spraying" (LPPS). The chamber pumping system can regulate an operating pressure down to 1 mbar with a total gas flow of up to 140 SLPM. For the present study the torch current and voltage were 1500 A and 43 V respectively, and the pressure range was 2 – 10 mbar with 3/100 SLPM H<sub>2</sub>/Ar. The gun is mounted on a displacement system.

A modified enthalpy probe system, supplied by Tekna Plasma Systems [11], is used for the diagnostics of the expanding plasma plume at low pressure. It is based on the common atmospheric enthalpy probe system with the addition of a roots pump and the enlargement of the probe tip and pumping pipe dimensions in order to achieve the necessary gas sampling throughput at reduced pressure. The probe tip inner, outer diameter and length are 10, 20, 300 mm respectively, which is the best compromise between gas sampling efficiency and spatial resolution, since the diameter of the plasma jet exceeds 200 mm.

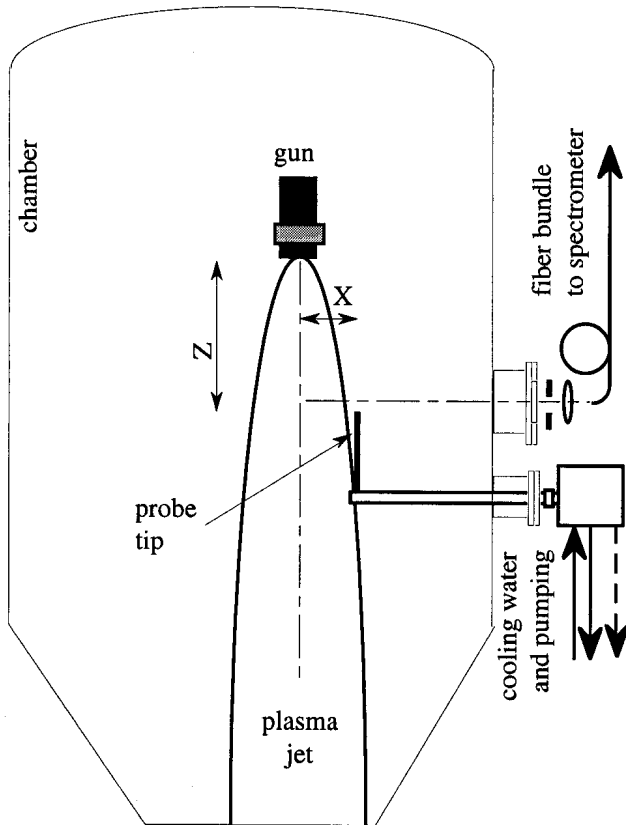


Figure 1: Drawing of the experimental arrangement (not to scale), showing the vacuum vessel with the enthalpy probe and the jet light collection for optical emission spectroscopy. X and Z refer to the probe-to-nozzle radial and axial distances, respectively.

The probe cooling water flow rate is also increased to account for the higher heat load on the large probe tip (up to 7 kW). The probe bulkhead is also larger than the standard one and is equipped with a separate cooling circuit because it is partially immersed in the plasma jet whose length can exceed 2 meters. The probe tip outer surface is covered with TBC to reduce the heat load in the "tare" mode with respect to the "sampling" mode [7]. The system is able to sample sufficient plasma gas to achieve a reliably measurable heat load difference between the "tare" and "sampling" condition [7] for chamber pressure down to 2 mbar. This is for sampling location at the jet fringes where the dynamic pressure due to the jet velocity of the does not assist the sampling of the plasma gas. Inside the jet, the dynamic pressure on the probe tip can be up to four times the static chamber pressure depending on the operation conditions, which makes the measurement more reliable as the probe approaches the jet axis. Figure 2 shows the probe inside the plasma jet at 6 mbar.

Optical emission spectroscopy of the plasma jet has been performed at about 30 mm above the probe tip end. The jet light is collected through a chamber window and an aperture and focused by a lens onto a fiber optic bundle. Light is then fed into the entrance slit of an ARC SP275 spectrometer which is fitted with a 1200 grooves/mm holographic grating and a TE cooled CCD detector. The spectral resolution is better than 0.1 nm, and the relative spectral transmittance of the system has been calibrated with a spectral radiance standard.

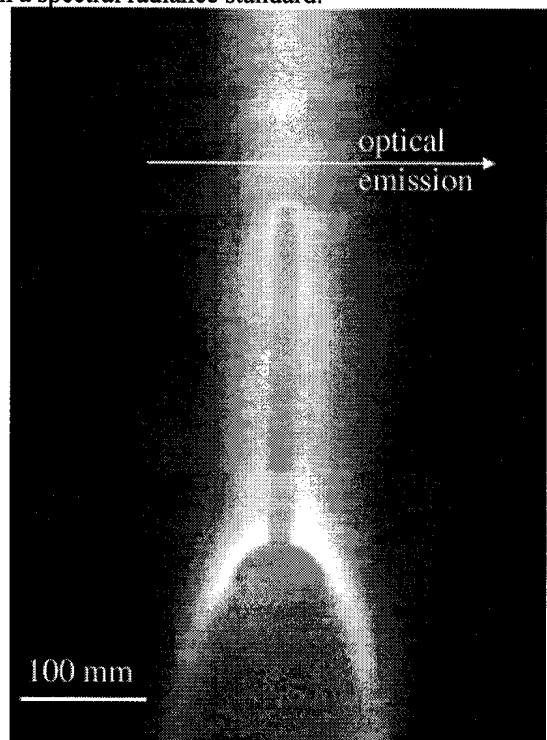


Figure 2 : Image of the probe on axis of the plasma jet at Z= 670 mm for a 6 mbar chamber pressure. The arrow indicates the optical emission collection path.

Enthalpy and optical emission measurements have been performed at various positions inside the plasma jet, in the range  $Z = 600 - 1000$  and  $X = 0 - 80$  mm (see Fig. 1).

### Results from enthalpy probe measurements

#### Axial profiles :

Figure 3 shows axial profiles along the jet axis of the specific enthalpy and of the local heat flux for three chamber pressures. The heat flux is obtained from the product of the calculated enthalpy, density and velocity. From Figure 3a one can see that the specific enthalpy is strongly dependent on the operating pressure and that it increases as the pressure decreases. The enthalpy at 2 mbar reaches up to 17 MJ/kg. The local heat flux is not monotonic as a function of pressure, and shows a maximum at 6 mbar. This is because it depends not only on the enthalpy but also on the density and jet velocity (see below). Moreover, at the axial distance where this measurement is performed, the probe is almost at the end of the 10 mbar plasma jet, whose length is much shorter than for the lower pressure cases. This is shown by the drop in the heat flux on Fig. 3b and the temperature on Fig. 4a as the axial distance is increased.

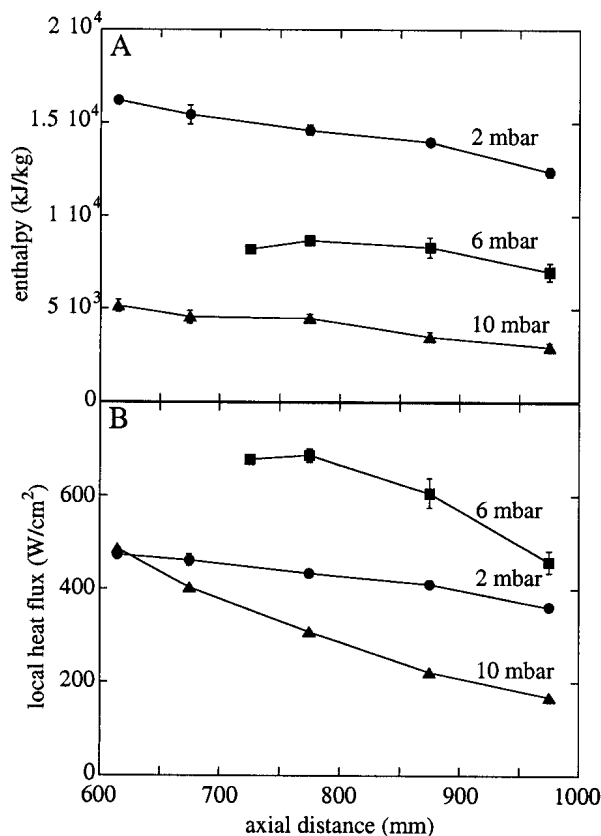


Figure 3 : Axial profiles on jet axis of the specific enthalpy (a) and of the local heat flux (b) for 3 chamber pressures.

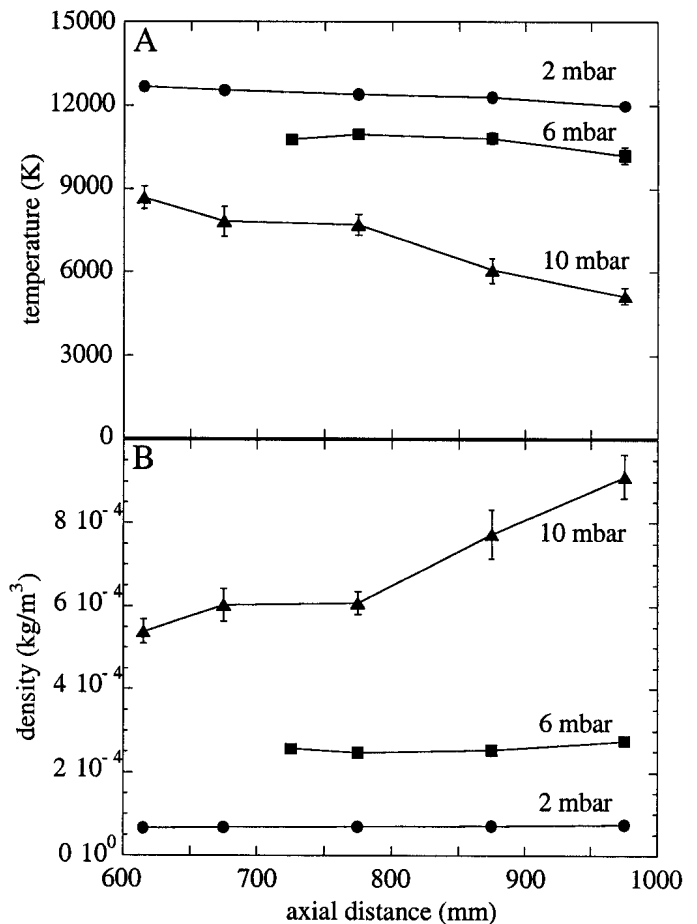


Figure 4 : Axial profiles on jet axis of the temperature (a) and of the density (b) for 3 chamber pressures.

This effect is not observed for the 2 and 6 mbar plasmas for which the plasma jet goes much farther than 1 m.

On Figure 4b the calculated density profiles basically show the inverse dependence of temperature.

#### Velocity calculation :

Since at these low pressures the flow cannot be considered as incompressible, compressible theory has to be used for the calculation of the jet velocity from the stagnation pressure at the probe tip in the "tare" mode ( $p_d$ ) and the static pressure measured at the chamber wall ( $p_\infty$ ) [9]. We assume an isentropic, frozen composition stagnation process [10]. For subsonic flow the Mach number ( $M$ ) is related to the ratio of the dynamic and static pressures ( $p_d/p_\infty$ ) by :

$$M < 1 : \frac{p_d}{p_\infty} = \left[ 1 + \left( \frac{\gamma - 1}{2} \right) M^2 \right]^{(\gamma/\gamma - 1)} \quad (1)$$

where  $\gamma = C_p/C_v$ , is the ratio of specific heats.

For supersonic flow we have :

$$M > 1 : \frac{P_d}{P_\infty} = \frac{\gamma + 1}{2} M^2 \left[ \frac{(\gamma + 1)^2 M^2}{4\gamma M^2 - 2\gamma + 2} \right]^{(1/\gamma - 1)} \quad (2)$$

The velocity ( $v$ ) is given by :

$$v = M \sqrt{\gamma R T} \quad (3)$$

with  $T$  being the local temperature and  $R$  the universal gas constant.

Figure 5 shows the jet velocity and the corresponding sound velocity axial profiles for three operation pressures. For 2 and 6 mbar the flow is clearly supersonic up to 1 meter from the nozzle exit, whereas for the 10 mbar case it becomes subsonic from about 0.6 meter from the nozzle exit. In addition, note that the velocity is almost constant over the axial distance investigated for the 2 mbar case.

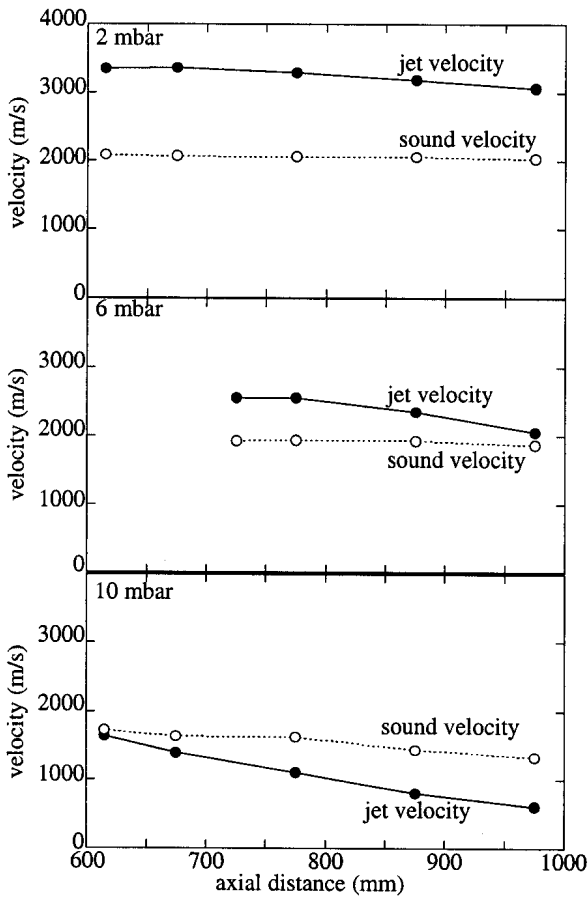


Figure 5 : Axial profiles on the jet axis of the measured velocity (-) and of the corresponding sound velocity (-) for 3 chamber pressures.

To summarize, it is observed that for very low pressure (2 mbar) the jet properties are almost constant over a quite large distance from the nozzle exit. This is because the surrounding gas density is very low and interacts only weakly with the jet. Moreover the mean free path is strongly increased and the collision frequency drastically reduced at these low pressures. The flow is laminar (Reynolds number in the range of 100) and the jet is only weakly cooled, or slowed down by the surrounding atmosphere.

**Radial profiles :**

Figure 6 shows radial profiles of the specific enthalpy and of the calculated local heat flux taken at 775 mm from the torch nozzle exit for three different operation pressures. For the 2 and 6 mbar cases, the profiles are more peaked as the pressure increases, whereas this trend is reversed for the 10 mbar case. This is because at 10 mbar the probe is nearly at the end of the plasma plume, where it diverges (see also Fig. 3 and 4 above).

Moreover at the end of the jet, there are fluctuations which tend to artificially broaden the average jet profile for the long time measurements performed with an enthalpy probe system.

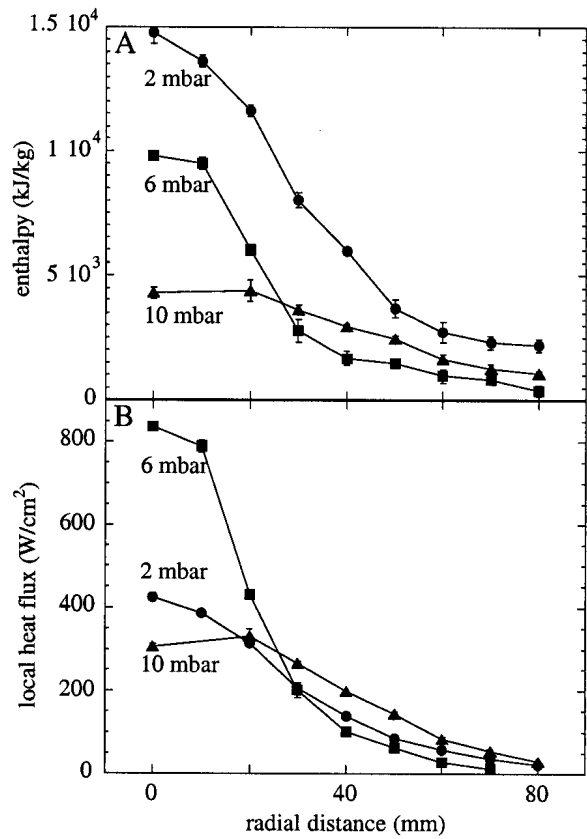


Figure 6 : Radial profiles at 775 mm from the torch nozzle exit of the specific enthalpy (a) and of the local heat flux (b) for 3 chamber pressures.

Figure 7 shows the calculated temperature and density profiles at the same axial position as for Fig. 6. As already shown and discussed in Fig 4, the temperature on axis is higher at low pressure. The same effect of profile broadening of enthalpy and heat flux at 10 mbar (Fig. 6) is also observed for the temperature here. The effect of pressure on jet broadening is particularly evidenced by the density profiles at 2 and 6 mbar, which differ by almost one order of magnitude at the jet fringe, and by only about a factor of 2.5 on jet axis.

The calculated velocity radial profiles are presented in Figure 8, along with the corresponding sound velocity for three pressures. The flow is supersonic close to axis for the two lower pressures, and becomes subsonic towards the edge of the jet. This transition occurs at a radius of about 50 mm at 2 mbar and 30 mm at 6 mbar. The flow is clearly subsonic for the 10 mbar case at this axial distance, but it might be also supersonic closer to the nozzle (see Fig. 5). We were unable to perform measurements at distances closer than 620 mm because of the excessive heat load to the bulkhead. The system will be modified in the future to account for this lack of cooling.

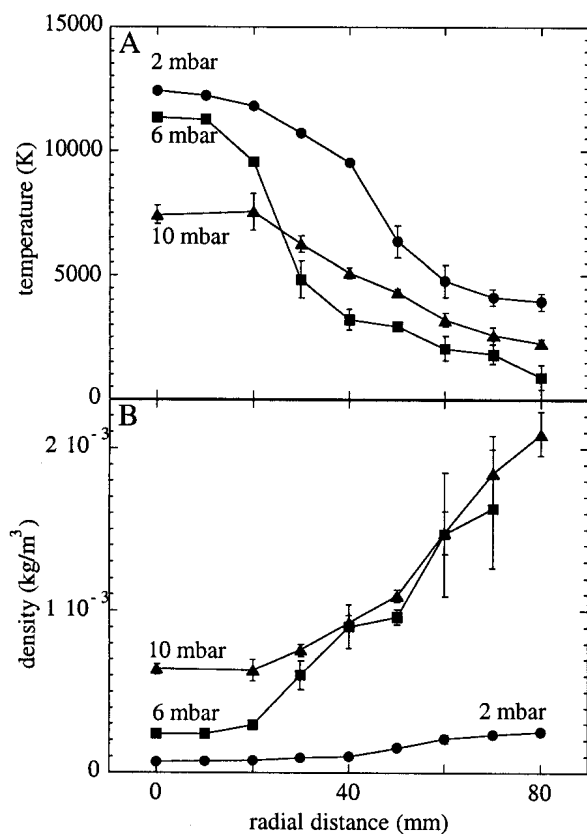


Figure 7 : Radial profiles at 775 mm from the torch nozzle exit of the temperature (a) and of the density (b) for 3 chamber pressures.

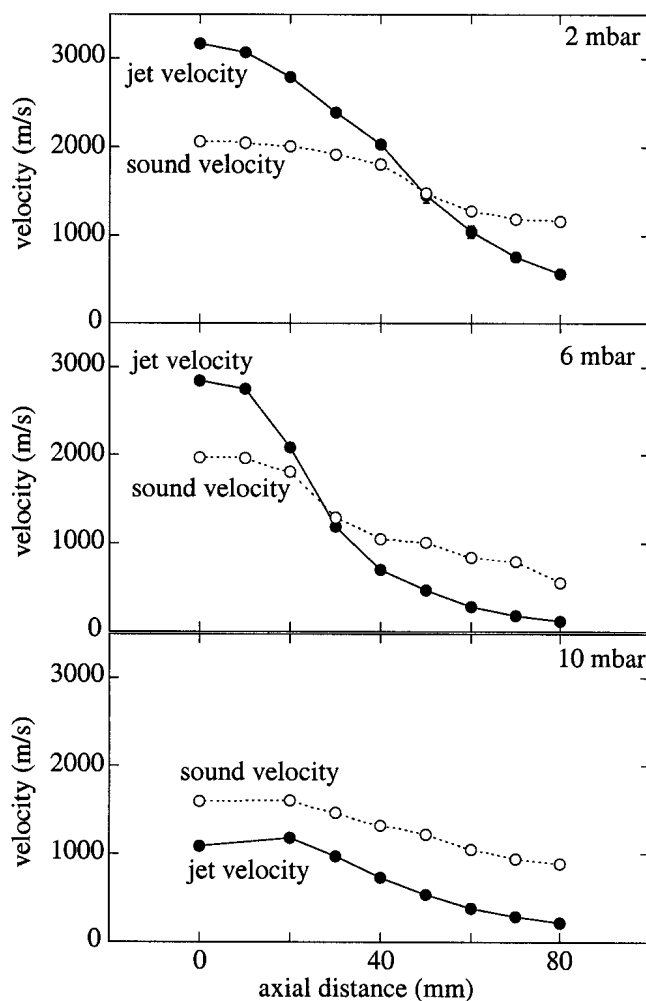


Figure 8 : Radial profiles at 775 mm from the torch nozzle exit of the measured velocity (-) and of the corresponding sound velocity (--) for 3 chamber pressures.

### Optical emission spectroscopy

Figure 9 show a comparison of optical emission spectra of plasma jets operating at atmosphere (APS) and at low pressure (6 mbar). The measurement has been taken on the jet axis at about 1/3 of its length from the nozzle exit. The spectral resolution is the same for both spectra (0.1 nm). A striking difference is the absence of continuum emission for the low pressure plasma which is the sign of absence of recombination due to the lack of collisions. Another main difference is the peak widths, which are reduced by more than a factor of two at low pressure. The reason for this is also the reduced collision rate and also the reduced plasma density: collisional and Stark broadening, which are the dominant broadening mechanisms at atmospheric pressure, then become less effective at low pressure.

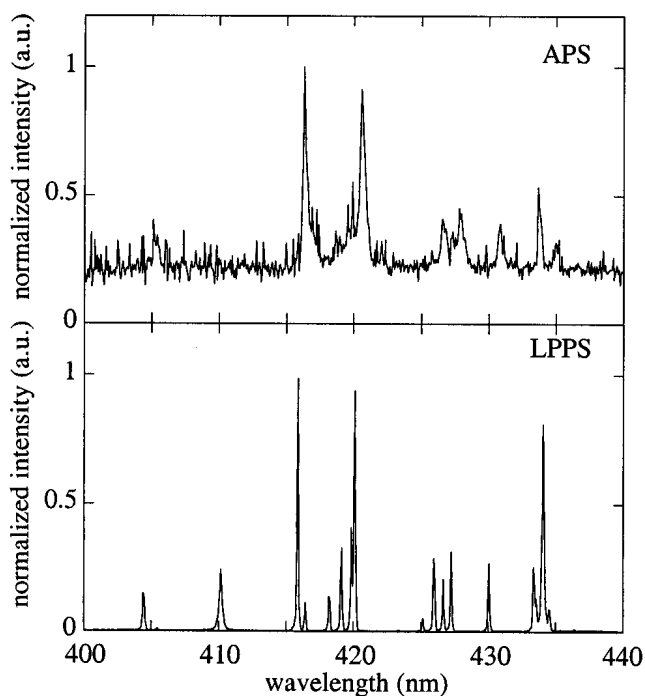


Figure 9 : Comparison of optical emission spectra taken on axis of the jet for an APS plasma and for an LPPS plasma at 6 mbar. Spectral resolution 0.1 nm.

### Summary and Conclusions

Preliminary measurements of plasma jet properties for a DC plasma gun operated below 10 mbar have been performed using a modified enthalpy probe system and optical emission spectroscopy. The results show that this new kind of expanding plasma jet is governed by physical mechanisms different from the ones which prevail in atmospheric thermal jets. In particular, the low collision rate between the various plasma species, due to the low density, is responsible for the large dimensions of the jet, for the spatial uniformity of its properties and for the deviation from local thermodynamic equilibrium. The flow is supersonic over nearly the entire jet volume and the influence of turbulence is weakened. Since these low pressure jets are no longer in local thermodynamic equilibrium, further work is necessary to account for the low pressure effect on thermodynamic and transport properties. Moreover other kinds of diagnostics will have to be used, such as laser scattering, in order to validate enthalpy probe measurements.

### Acknowledgments

The authors are grateful to Prof. M. Boulos and E. Bouchard from Tekna Plasma Systems Inc. for their interest in this work.

### References

1. P. Fauchais and M. Vardelle, "Plasma Spraying: Present and Future", Pure and Appl. Chem., Vol. 66, No. 6, p. 1247-1258, (1994)
2. E. Muehlberger, "Method of Forming Uniform Thin Coatings on Large Substrates", US Patent 5.853.815, December 1998.
3. M. Loch, and G. Barbezat, "Characteristics and Potential Application of Thermally Sprayed Thin Film Coatings", "Thermal Spray: Surface Engineering via Applied Research", Ed. C. C. Berndt, Pub. ASM International, Material Park, OH, USA, 1141, (2000).
4. N. Singh, M. Razafinimanana, and A. Gleizes, "The effect of pressure on a plasma plume: temperature and electron density measurements", J. Phys. D: Appl. Phys. 31, 2921, (1998).
5. H. J. Kim and S. H. Hong, "Comparative measurements of thermal plasma jet characteristics in atmospheric and low pressure plasma spraying", IEEE Transactions on Plasma Science 23 (5), 852, (1995).
6. M. C. M. van de Sanden, R. J. Severens, W. M. M. Kessels, R. F. G. Meulenbroeks and D. C. Schram, J. Appl. Phys. 84, 2426, (1998); J. Appl. Phys. 85, 1243, (1999) and references therein.
7. M. Rhamane, G. Soucy, and M. I. Boulos, "Analysis of the enthalpy probe technique for thermal plasma diagnostics", Rev. Sci. Instrum. 66 (6), 3424, (1995).
8. A. Capetti and E. Pfender, "Probe measurements in argon plasma jets operated in ambient argon", Plasma Chemistry and Plasma Processing 9 (2), 329, (1989).
9. M. Hollenstein, M. Rhamane, and M. I. Boulos, "Aerodynamic study of the supersonic induction plasma jet", Proc. of the 14<sup>th</sup> Int. Symposium on Plasma Chemistry, Prague, Czech Republic, p.257, (1999).
10. J. R. Fincke, W. D. Swank, S. C. Snider, and D. C. Haggard, "Enthalpy probe performance in compressible thermal plasma jets", Rev. Sci. Instrum. 64 (12), 3585, (1993).
11. Tekna Plasma Systems Inc., 3535 Boul. Industriel, Sherbrooke, Québec, Canada.